SLAC-PUB-8857
June, 2001

Impedance of Small-Angle Collimators in High-Frequency Limit*

G. V. Stupakov
Stanford Linear Accelerator Center, Stanford University, Stanford, CA 94309

Abstract

We consider round an rectangular-aperture tapered collimators with a small taper angle α. Depending on the angle, aperture, and the frequency different parameter regimes are found with specific scalings of the impedance. The physical mechanism involved in formation of the beam wake field is discussed. Analytical formulas are derived for the limiting case of the diffraction regime for round collimators. For rectangular geometry with a large width to height ratio, two new regimes — diffraction and intermediate – are found and the impedance is calculated for each regime. In addition to consideration based on solution of Maxwell's equations, a simple recipe is given for calculation of the impedance in the diffraction regime for both round and rectangular geometries.

*Work supported by Department of Energy contract DE–AC03–76SF00515.

1 Introduction

Collimators are often used in storage rings and accelerators to remove high-amplitude particles from the transverse profile of the beam. Being close to the beam orbit they may introduce large impedance that perturbs the beam motion downstream of the collimator and results in additional emittance growth and jitter amplification of the collimated beam. The wake effect of the collimators is of concern for future colliders, such as the Next Linear Collider [1], with extremely small transverse emittance of the beam.

To lower the collimator impedance one can try to taper the collimator jaws to get a gradual transition from a large to a small aperture and back. Two examples of such collimators – a round and a rectangular one – are shown in Fig. 1.

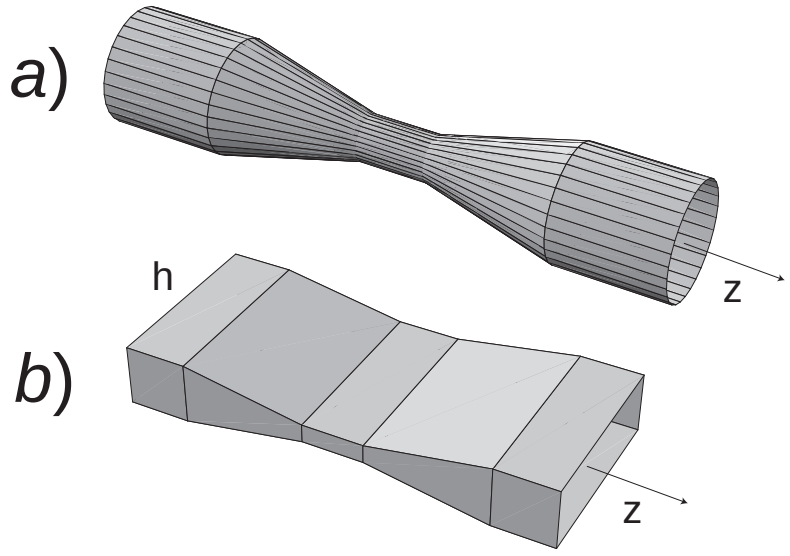

Figure 1: Geometry of a round (a) and a rectangular (b) tapered collimators. For the rectangular collimator, h denotes its width in the horizontal plane.

The impedance of a smooth round tapered transition was calculated by K. Yokoya in the limit of low frequencies [2]. For the transverse impedance, Yokoya's formula gives

$$Z_t = -\frac{iZ_0}{2\pi}\int dz \left(\frac{b'}{b}\right)^2, \qquad (1)$$

where $b(z)$ is the radius of the collimator as a function of longitudinal coordinate z, $Z_0 = 377$ Ohm, and the prime denotes the derivative with respect to z. It was shown later [3] that the condition of applicability of Yokoya's formula is

$$\alpha k b \ll A, \tag{2}$$

where α is the angle of the collimator, b is the minimal radius, $k = \omega/c$, and A is a numerical factor of order of unity. For a bunch of length σ_z, the characteristic value of k in the beam spectrum is equal to σ_z^{-1}.

A generalization of Yokoya's result for a rectangular collimator of large aspect ratio, $h \gg b$, was given in Ref. [4]. The vertical transverse impedance in this case is given by the following formula

$$Z_t = -\frac{iZ_0 h}{2} \int dz \frac{(b')^2}{b^3}, \tag{3}$$

where $b(z)$ is the half-gap of the collimator and h is its width. Eq. (3) shows that the impedance of a flat collimator with a large value of h is higher than the impedance of a round collimator with the same function $b(z)$ – a result that seems surprising if one considers the limit $h \to \infty$. It turns out however, that the applicability condition of Eq. (3) is

$$\frac{\alpha k h^2}{b} \ll 1. \tag{4}$$

It is much tighter than Eq. (2) and means that Eq. (3) is not applicable for very large values of h. Unfortunately, the condition (4) was not formulated in the original publication [4], and in some cases resulted in the use of Eq. (3) beyond its applicability limits.

In this paper we will give a classification of possible regimes for impedance of both round and rectangular tapered collimators and will discuss the physical mechanisms involved into the formation of the beam wake field. We will also calculate the impedance of such collimators for the angles that do not satisfy the conditions (2) and (4). Note that we are only interested here in the case of short bunches, $\sigma_z \ll b$, and ultrarelativistic energies, $\gamma \to \infty$.

The comparison of theoretical results obtained in this paper with recent measurements of the collimator wake at SLAC [5] can be found in a companion paper [6].

2 Classification of possible regimes

First, consider a beam propagating in a straight round perfectly conducting pipe of a constant radius. For impedance calculations, it is convenient to assume a Fourier transform of the beam current $I_\omega = I_0 e^{ikz-i\omega t}$, where I_0 is the amplitude of the current. The current density $j_{\rm im}$ of the image current on the wall will have the same dependance $j_{\rm im} \sim e^{ikz-i\omega t}$, which means that the image current propagates with the speed of light. Since electromagnetic waves in a straight pipe have a phase velocity greater than the speed of light, the wall currents do not excite these modes, hence, the beam does not radiate. This explains why impedance vanishes in a straight perfectly conducting pipe.

Now, assume a round tapered collimator of length $l \sim b/\alpha$ with a perfectly conducting wall. Because of the variation of the pipe radius, the image current acquires an additional factor $f(z)$, $j_{\rm im} \sim f(z)e^{ikz-i\omega t}$, where $f(z)$ is a smooth function that varies on the scale of variation of the taper radius l. Making now Fourier decomposition of $j_{\rm im}$ with respect to z, we find a spectrum of width $\Delta k \sim l^{-1}$. Because of this broadening, there will be harmonics in the spectrum of $j_{\rm im}$ with the phase velocity $v_{\rm ph}$ exceeding the speed of light. It is easy to see that by order of magnitude $|v_{\rm ph} - c| \sim c^2\Delta k/\omega \sim c/lk$. Comparing $v_{\rm ph}$ with the lowest phase velocity $c(1 + j_{01}^2/k^2b^2)^{1/2}$ of TM modes in a round pipe, we find that the radiation begins if

$$\frac{kb^2}{l} = kb\alpha \gtrsim j_{01}^2. \tag{5}$$

This condition, by order of magnitude, is opposite to Eq. (2) which explains why the impedance in Eq. (1) is purely inductive — in the regime given by Eq. (2) the beam does not radiate, and hence, does not lose energy.

We will call the regime of parameters where Eq. (5) is satisfied the *diffraction* regime. The impedance in this regime is calculated in Sections 5 and 6.

The same consideration is also applicable for a rectangular collimator with a large aspect ratio. An important difference, however, is that the lowest phase velocity of TE_{0n} eigenmodes in rectangular cross-section waveguide is equal to $c(1 + \pi^2/k^2h^2)^{1/2}$. Hence, the radiation occurs when

$$\frac{kh^2}{l} = \frac{kh^2\alpha}{b} \gtrsim \pi^2. \tag{6}$$

When this equation is satisfied the regime of purely inductive impedance Eq. (3) breaks down. This is in agreement with the fact that the applicability condition Eq. (4) is opposite to Eq. (6). If the angle of the collimator is such that Eq. (6) is satisfied, but $kb\alpha \ll 1$, only a limited number of TE_{0n} will be excited. We will call this regime *intermediate* to indicate that it is located in the parameter space between the inductive regime and the diffraction one.

Finally, when $kb\alpha$ is greater than unity, the rectangular collimator is in the diffraction regime, and one can expect the wake of the rectangular collimator similar to the wake of the round collimator in the diffraction regime.

Calculation of the impedance for rectangular collimator is described in Section 8.

3 The Method

We will use a method that was previously employed in other problems [7] for calculation of the impedance in a perfectly conducting environment. In this method, the radiation of the image currents induced by the beam in the wall is calculated. In the absence of other losses, the radiated energy is equal to the energy loss of the beam and can be related to the real part of the impedance. The imaginary part of the impedance can then be found using the Kramers-Kronig relation. In this section, the method is formulated for the simplest case of the longitudinal impedance of a round taper. The actual calculation of the longitudinal impedance in this case is carried out in Section 5. With a slight modification, the method will also be applied for the transverse impedance both in cylindrical and rectangular geometries in Sections 6 and 8 .

The geometry of a round conical taper is shown in Fig. 2. We will use two coordinate systems inside the taper – a cylindrical coordinate system ρ, ϕ and z, and a spherical coordinate system r, θ, ϕ, with the center of the spherical system located at the vertex of the cone. The taper connects two round pipes of radii b_1 and b_2, $b_2 > b_1$. The taper angle α is assumed to be small, $\alpha \ll 1$.

The Fourier component of frequency ω of the beam current is (we assume the $e^{-i\omega t}$ time dependence in what follows)

$$I_\omega = I_0 e^{ikz}, \tag{7}$$

where I_0 is the amplitude of the current harmonic and $k = \omega/c$. Denote

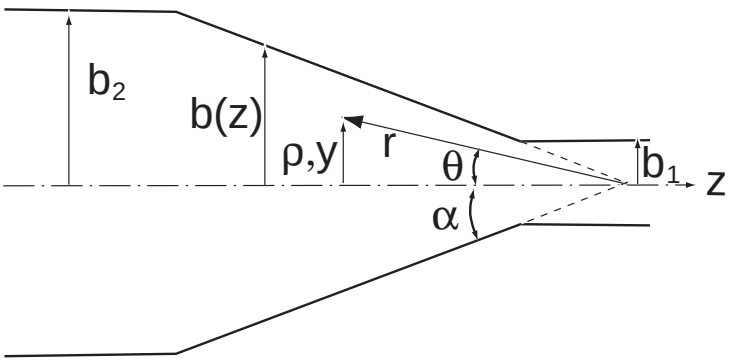

Figure 2: A taper of the collimator with coordinate systems. The distance from the axis is measured by the radius vector ρ in cylindrical geometry and by the coordinate y for a rectangular collimator.

by P_ω the averaged over time intensity of radiation of this current from the collimator region. The real part of the impedance is given by the following relation (see, e.g. [8])

$$\mathrm{Re}\, Z(\omega) = \frac{2P_\omega}{I_0^2}. \tag{8}$$

The radiation is due to the image currents induced in the perfectly conducting walls in the region where they are not parallel to the z-axis. It is convenient to represent the total electric field of the beam current (7) inside the taper as a sum of the vacuum field, $\boldsymbol{E}^{\mathrm{vac}}$, and the radiation field $\boldsymbol{E}^{\mathrm{rad}}$,

$$\boldsymbol{E} = \boldsymbol{E}^{\mathrm{vac}} + \boldsymbol{E}^{\mathrm{rad}}, \tag{9}$$

where for an on-axis beam

$$\boldsymbol{E}^{\mathrm{vac}} = \hat{\boldsymbol{\rho}} \frac{2I_0}{\rho c} e^{ikz}, \tag{10}$$

with $\hat{\boldsymbol{\rho}}$ being a unit vector in the radial direction of the cylindrical coordinate system.

The radiation field $\boldsymbol{E}^{\mathrm{rad}}$ satisfies Maxwell's equation with the boundary condition that requires the tangential component of the total electric field on the wall to vanish

$$\boldsymbol{E}_t^{\mathrm{rad}}|_{\mathrm{wall}} = -\boldsymbol{E}_t^{\mathrm{vac}}|_{\mathrm{wall}}. \tag{11}$$

A powerful method of solution of Maxwell's equations with the boundary condition given by Eq. (9) is given by Vainshtein [9] (see also [10]). In this method, a non-vanishing tangential component of the electric field on the wall is replaced by the surface magnetic current $\boldsymbol{i}^{\rm mag}$ located *inside* the waveguide infinitesimally close to the wall. The magnitude and the direction of the magnetic current is

$$\boldsymbol{i}^{\rm mag} = \frac{c}{4\pi}\boldsymbol{n} \times \boldsymbol{E}_t^{\rm rad}|_{\rm wall} = -\frac{c}{4\pi}\boldsymbol{n} \times \boldsymbol{E}_t^{\rm vac}|_{\rm wall}, \tag{12}$$

where $\boldsymbol{n}$ is the unit vector normal to the surface and directed toward the metal. Note that the magnetic current exists only inside the taper and vanishes in the region where the wall is parallel to the z axis.

Inside the waveguide, the radiation field excited by the magnetic currents can be represented as a sum of eigenmodes

$$\boldsymbol{E}^{\rm rad} = \sum_n a_n^+ \boldsymbol{E}_n^+ + \sum_n a_n^- \boldsymbol{E}_n^-, \tag{13}$$

where $a_n^\pm$ is the amplitude and $\boldsymbol{E}_n^\pm$ is the electric field of the n-th eigenmode, and the sign indicates that the wave propagates in the positive (+) or negative (−) direction of the z axis. A similar expansion in terms of the amplitudes $a_n^\pm$ is also valid for the magnetic field.

In the region occupied by the radiated current (inside the taper), the amplitudes $a_n^\pm$ are functions of the coordinate z. However, for calculation of the radiated power we only need expressions for the field far from the collimator area. In this region, the amplitudes $a_n^\pm$ are given by the following integrals [9]

$$a_n^+ = -\frac{1}{N_n}\int \boldsymbol{i}^{\rm mag} \cdot \boldsymbol{H}_n^- dS, \qquad a_n^- = -\frac{1}{N_n}\int \boldsymbol{i}^{\rm mag} \cdot \boldsymbol{H}_n^+ dS, \tag{14}$$

where $\boldsymbol{H}_n^\pm$ is the magnetic field of the n-th eigenmode and the integration covers the area occupied by the magnetic current. The norm N_n of the mode n in Eq. (14) is defined as

$$N_n = \frac{c}{4\pi}\int d\boldsymbol{S}\left(\boldsymbol{E}_n^+ \times \boldsymbol{H}_n^- - \boldsymbol{E}_n^- \times \boldsymbol{H}_n^+\right), \tag{15}$$

where the integral is taken over the cross section of the waveguide. Properly defined eigenmodes are orthogonal with the norm given by Eq. (15).

The energy radiated by the current P_ω can be written as a sum over all possible modes,

$$P_\omega = \sum_n P_n(|a_n^+|^2 + |a_n^-|^2), \tag{16}$$

where P_n is the energy flow in the mode of unit amplitude.

4 Eigenmodes in Small-Angle Conical Taper

Eigenmodes in a conical taper can be divided into TE and TM modes [9], similar to the classification of modes in a circular waveguide. In a spherical coordinate system shown in Fig. 2, TE modes have $E_r = 0$, and TE modes are characterized by $H_r = 0$.

Consider first axisymmetric TM_{0n} modes in a conical taper with angle α. Approximate formulas for the electric and magnetic fields in the n-th mode valid in the limit $\alpha \ll 1$ are given by

$$\begin{aligned} E_r &= \frac{\nu^2}{r^2} J_0(\nu\theta)\sqrt{x} H_\nu(x), \\ E_\theta &= -\frac{\nu k}{r} J_1(\nu\theta)(\sqrt{x} H_\nu(x))', \\ H_\phi &= -\frac{i\nu k}{r} J_1(\nu\theta)\sqrt{x} H_\nu(x), \end{aligned} \tag{17}$$

where r, θ and ϕ are the spherical coordinates, $x = kr$, the prime denotes differentiation with respect to x, $\nu = j_{0n}/\alpha$ with j_{0n} being the n-th root of the Bessel function J_0, and J_1 is the Bessel function of the first order. The function H_ν is the Hankel function of the order ν, and for waves propagating in the positive or negative z-direction (see Fig. 1) H_ν is the second order $H_\nu^{(2)}$ or the first order $H_\nu^{(1)}$, respectively.

The norm of the n-th mode can be found by direct integration of Eq. (15) and is given by

$$N_n = ck^2 \frac{j_{0n}^2}{\pi} \left[(1 - j_{0n}^{-2}) J_1^2(j_{0n}) + \frac{1}{4} J_2^2(j_{0n}) \right]. \tag{18}$$

In the limit of $n \gg 1$,

$$N_n \approx 2ck^2 \frac{n}{\pi}. \tag{19}$$

The energy flow P_n (equal to the integrated over the cross section averaged over the time Poynting vector) in the mode is $P_n = \frac{1}{4}N_n$.

For the transverse impedance we will need the dipole modes TM_{1n} and TE_{1n}. The TM_{1n} modes in the limit $\alpha \ll 1$ are given by

$$\begin{aligned} E_r &= \frac{\nu^2}{r^2} J_1(\nu\theta)\sqrt{x}H_\nu(x)\sin\phi, \\ E_\theta &= \frac{\nu k}{r} J_1'(\nu\theta)(\sqrt{x}H_\nu(x))'\sin\phi, \\ E_\phi &= \frac{k}{r\theta} J_1(\nu\theta)(\sqrt{x}H_\nu(x))'\cos\phi, \\ H_\theta &= -\frac{ik}{r\theta} J_1(\nu\theta)\sqrt{x}H_\nu(x)\cos\phi, \\ H_\phi &= \frac{i\nu k}{r} J_1'(\nu\theta)\sqrt{x}H_\nu(x)\sin\phi, \end{aligned} \tag{20}$$

where $\nu = j_{1n}/\alpha$ and j_{1n} is n-th root of the Bessel function J_1. As above, H_ν is the Hankel function of the order ν equal to $H_\nu^{(2)}$ for the forward waves and $H_\nu^{(1)}$ for the backward waves. The norm of a TM_{1n} mode is

$$N_n = ck^2 \frac{j_{1n}^2}{8\pi} \left[J_0(j_{1n}) - J_2(j_{1n})\right]^2, \tag{21}$$

which for $n \gg 1$ reduces to $N_n = ck^2 n/\pi$. The energy flow in the mode is $P_n = \frac{1}{4}N_n$.

The field of a TE_{1n} mode can be formally obtained from Eqs. (20) by the following transformation: $E_r^{\mathrm{TM}} \to H_r^{\mathrm{TE}}$, $E_\theta^{\mathrm{TM}} \to H_\theta^{\mathrm{TE}}$, $E_\phi^{\mathrm{TM}} \to H_\phi^{\mathrm{TE}}$, $H_\theta^{\mathrm{TM}} \to -E_\theta^{\mathrm{TE}}$, $H_\phi^{\mathrm{TM}} \to -E_\phi^{\mathrm{TE}}$ (and $E_r^{\mathrm{TE}} = 0$). The factor ν in Eq. (20) for the TE_{1n} modes becomes $\nu = j'_{1n}/\alpha$, where j'_{1n} is the n-th rood of the derivative of the Bessel function J_1'. The norm for those modes is negative,

$$N_n = -ck^2 \frac{1}{2\pi} (j'^2_{1n} - 1) J_1^2(j'_{1n}), \tag{22}$$

and the energy flow in the mode is $P_n = -\frac{1}{4}N_n$. For large n, approximately, $N_n = -ck^2 n/\pi$.

The eigenmodes given above are only valid in conical regions of the collimator. For our purposes, the eigenmodes have to be extended into the regions of straight pipes adjacent to the taper and defined for $-\infty < z < \infty$. In the general case of an arbitrary angle α finding the field of the modes outside of the taper would require a proper matching of the conical eigenmodes

with the eigenmodes in cylindrical pipes. Reflection and mode conversion in the transition regions would couple modes with different n propagating both in negative and positive directions. Fortunately, in the limit $\alpha \ll 1$ the reflection and conversion effects are small, and the problem is greatly simplified. In this case, in the zero order approximation, one can assume that a TM_{mn} (TE_{mn}) mode in the conical region propagates as a corresponding TM_{mn} (TE_{mn}) mode of the same amplitude in the straight pipe. Using the relation $\nu\theta = j_{0n}\theta/\alpha \approx j_{0n}\rho/b$, it is easy to see that the radial structure of modes (17) is about the same as the radial dependence in TM_{0n} modes in a straight cylindrical pipe. The same is true for the dipole modes given by Eq. (20).

As we will see below, at high frequency, the modes are radiated by the beam at small angle to the axis. They propagate through the collimator region without being reflected from the narrow part of the taper. This means that we only need the modes with the frequencies much higher than the cutoff frequency.

5 Longitudinal impedance of a conical collimator in diffraction regime

For calculation of the longitudinal wake we will assume that the beam current given by Eq. (7) is located on the axis, and will calculate the radiation coming out from the entrance taper of the collimator, shown in Fig. 2.

In the spherical coordinate system, the tangential electric field of the vacuum field on the wall has only radial component, $E_r^{\mathrm{vac}} = E_\rho^{\mathrm{vac}} \sin\alpha \approx (2I_0\alpha/\rho c)e^{ikz}$, which, according to Eq. (12) can be represented by the azimuthal magnetic current

$$i_\phi^{\mathrm{mag}} = \frac{I_0}{2\pi r} e^{-ikr\cos\alpha}, \tag{23}$$

where we have used the relation $\rho \approx \alpha r$ and $z \approx -r\cos\alpha$. This current will only excite the TM_{0n} modes, with the amplitudes given by Eqs. (14). Since for large x, $H_\nu^{(1)}(x) \propto x^{-1/2}e^{ix}$ and $H_\nu^{(2)}(x) \propto x^{-1/2}e^{-ix}$, it is easy to see that the radiation in the backward direction is small, because a_n^- is given by an integral of a function with a rapidly oscillating phase $\propto e^{ikr(1+\cos\alpha)}$. The dominant radiation goes in the forward direction, and we need to evaluate

the amplitude a_n^+ only. Using Eqs. (14) and (17) we find

$$a_n^+ = \frac{ij_{0n}kI_0}{N_n} J_1(j_{0n}) \int_{x_1}^{x_2} \frac{dx}{\sqrt{x}} H_\nu^{(1)}(x) e^{-ix\cos\alpha}, \tag{24}$$

where $x_1 = kr_1$, $x_2 = kr_2$, and r_2 and r_1 are the values of the radius r at the entrance to and at the exit from the taper, see Fig. 2. The integral in Eq. (24) is calculated in the Appendix using the stationary phase method. As shown there, this method can be used in the diffraction regime, when Eq. (5) is satisfied. The result is

$$\int_{x_1}^{x_2} \frac{dx}{\sqrt{x}} H_\nu^{(1)}(x) e^{-ix\cos\alpha} \approx \begin{cases} 2(\alpha\nu)^{-1/2} e^{i\zeta_0}, & \text{for } x_1 < \frac{\nu}{\alpha} < x_2, \\ 0, & \text{for } \frac{\nu}{\alpha} < x_1 \text{ or } \frac{\nu}{\alpha} > x_2, \end{cases} \tag{25}$$

where ζ_0 is a phase that we will not need in what follows. According to Eq. (25), the modes that are radiated from the taper have numbers n such that $j_{0n} = \nu/\alpha > x_1 \gg 1$, hence $n \gg 1$. Using the asymptotic expression in the limit of large n: $N_n \approx 2ck^2 n/\pi$, $\nu/\alpha = j_{0n} \approx \pi n$, $|J_1(j_{0n})| \approx (2/\pi^2 n)^{1/2}$, we find

$$|a_n^+| \approx \frac{\sqrt{2\pi}}{ckn} I_0, \tag{26}$$

when n is in the range $n_1 < n < n_2$, where, from Eq. (25), $n_1 = x_1/\pi$ and $n_2 = x_2/\pi$. For the energy flow in the n-th mode we have

$$|a_n^+|^2 P_n \approx \frac{I_0^2}{cn}. \tag{27}$$

Because n is large, we can use integration over n to find the total radiated energy at frequency ω

$$P_\omega = \int_{n_1}^{n_2} dn\, |a_n^+|^2 P_n = \frac{I_0^2}{c} \ln\frac{n_2}{n_1} = \frac{I_0^2}{c} \ln\frac{b_2}{b_1}. \tag{28}$$

The radiation for the whole collimator is equal to twice the radiation from the taper, which gives for the real part of the longitudinal impedance of the collimator in the diffraction regime

$$\mathrm{Re}\, Z_l = 2\frac{P_\omega}{\frac{1}{2}I_0^2} = \frac{Z_0}{\pi} \ln\frac{b_2}{b_1}, \tag{29}$$

where $Z_0 = 4\pi/c = 377$ Ohm.

It is interesting to note that the radiated energy calculated above can be easily found from a simple geometro-optical argument. The incident electromagnetic field of the beam current in the annulus $b_1 < \rho < b_2$ impinges the lateral wall of the taper and is mirror reflected by the wall. This part of the beam field, after reflection, detaches from the beam charge and becomes converted into the radiation field. Hence the radiated power is equal to the incident energy flow in the region $b_1 < \rho < b_2$. Using Eq. (10), we can find the average Poynting vector of the vacuum field of the beam,

$$S = \frac{c}{8\pi}(E^{\rm vac})^2 = \frac{I_0^2}{2\pi c\rho^2}, \tag{30}$$

and calculate the energy flow in the annulus:

$$\int_{b_1}^{b_2} 2\pi\rho d\rho S = \frac{I_0^2}{c}\ln\frac{b_2}{b_1}, \tag{31}$$

which is exactly equal to the result given by Eq. (28).

6 Transverse impedance of conical collimator in diffraction regime

For calculation of the transverse wake, we consider a beam shifted from the axis in vertical direction by an infinitesimally small distance Δ. The transverse wake is due to the excitation of dipole modes in the waveguide. These modes are excited by the dipole momentum of the beam, and instead of considering an offset current, we can consider two currents of opposite sign, $I_0 e^{ikz}$ and $-I_0 e^{ikz}$, with the offsets $\Delta/2$ and $-\Delta/2$, respectively. The electric field of such a dipole current in the pipe of radius b_2, outside of the collimator, is

$$\boldsymbol{E}^0 = \frac{2I_0\Delta}{c}e^{ikz}\left[\frac{2\boldsymbol{\rho}(\hat{\boldsymbol{y}}\boldsymbol{\rho}) - \rho^2\hat{\boldsymbol{y}}}{\rho^4} + \frac{\hat{\boldsymbol{y}}}{b_2^2}\right], \tag{32}$$

where $\hat{\boldsymbol{y}}$ is the unit vector in the direction of the offset. The first term in the square brackets is the vacuum dipole field and the second term is the field generated by the image charges in the pipe.

To calculate the radiation from the taper for a dipole current, we need to modify the approach outlined in Section 3. Instead of using the vacuum

field $\boldsymbol{E}^{\rm vac}$ in Eq. (9) we will use the field $\boldsymbol{E}^0$ that the beam has in the pipe of radius b_2, so that $\boldsymbol{E} = \boldsymbol{E}^{\rm rad} + \boldsymbol{E}^0$. The advantage of such choice is that outside of the collimator, in the absence of radiation, the electric field $\boldsymbol{E}$ would be equal to $\boldsymbol{E}^0$, and hence the difference $\boldsymbol{E} - \boldsymbol{E}^0$ represents the "true" radiation coming out of the collimator.

Inside the taper the field $\boldsymbol{E}^0$ has both radial and azimuthal tangential components on the wall

$$\begin{aligned} E_r^0|_{\rm wall} &= \frac{2I_0\Delta\alpha}{c}\sin\phi\left(\frac{1}{b^2}+\frac{1}{b_0^2}\right)e^{ikz}, \\ E_\phi^0|_{\rm wall} &= -\frac{2I_0\Delta}{c}\cos\phi\left(\frac{1}{b^2}-\frac{1}{b_0^2}\right)e^{ikz}. \end{aligned} \tag{33}$$

As pointed out in Section 3, the solution of Maxwell's equations with the proper boundary condition can be obtained by introducing the magnetic currents (12):

$$\begin{aligned} i_\phi^{\rm mag} &= -\frac{I_0\Delta\alpha}{2\pi}\sin\phi\left(\frac{1}{b^2}+\frac{1}{b_0^2}\right)e^{ikz}, \\ i_r^{\rm mag} &= -\frac{I_0\Delta}{2\pi}\cos\phi\left(\frac{1}{b^2}-\frac{1}{b_0^2}\right)e^{ikz}. \end{aligned} \tag{34}$$

Consider first TM modes that are excited by the azimuthal magnetic currents $i_\phi^{\rm mag}$. Using Eq. (14) with magnetic field given by Eq. (20) we find

$$a_n^{+\rm TM} = \frac{ik^2\nu\Delta I_0}{2N_n}J_1'(j_{1n})\int_{x_1}^{x_2}dx\sqrt{x}\left(\frac{1}{x^2}+\frac{1}{x_2^2}\right)H_\nu^{(1)}(x)e^{-ix\cos\alpha}. \tag{35}$$

In the diffraction regime, the integral is evaluated in the Appendix. Analogously to the calculation of Section 5, we replace summation over n by integration and find for the total power radiated in TM modes

$$P_\omega^{\rm TM} = \frac{\Delta^2 I_0^2}{2cb_2^4}\int_{b_1}^{b_2}\frac{(b^2+b_2^2)^2}{b^3}db, \tag{36}$$

where b is the current pipe radius in the taper.

The TE modes are excited by both azimuthal and radial magnetic currents, however, the contribution due to the azimuthal current, which has an additional small factor α (see Eq. (34), is small and can be neglected.

A calculation similar to the one described above gives for the power in TE modes

$$P_\omega^{\mathrm{TE}} = \frac{\Delta^2 I_0^2}{2cb_2^4} \int_{b_1}^{b_2} \frac{(b^2 - b_2^2)^2}{b^3} db. \tag{37}$$

The total radiated power in all modes is

$$P_\omega = P_\omega^{\mathrm{TE}} + P_\omega^{\mathrm{TM}} = \frac{\Delta^2 I_0^2}{cb_2^4} \int_{b_1}^{b_2} \frac{b^4 + b_2^4}{b^3} db = \frac{\Delta^2 I_0^2 (1 - b_1^4/b_2^4)}{2cb_1^2}, \tag{38}$$

which gives for the real part of the longitudinal dipole impedance

$$\mathrm{Re}\, Z_l = \frac{2P_\omega}{I_0^2} = \frac{\Delta^2 (1 - b_1^4/b_2^4)}{cb_1^2}. \tag{39}$$

Using the Panofsky-Wentzel relation we can find the real part of the transverse impedance of the collimator

$$\mathrm{Re}\, Z_t = 2 \frac{1}{k\Delta} \frac{\partial \mathrm{Re}\, Z_l}{\partial \Delta} = \frac{4(1 - b_1^4/b_2^4)}{\omega b_1^2}, \tag{40}$$

where the factor of 2 takes into account the contribution of both tapers. Note that in this formula we neglected the contribution from the pipe of radius b_1 connecting the two tapers. This is valid if the connecting part is short enough.

Knowledge of the real part of the transverse impedance allows us to calculate the kick factor κ_t for a Gaussian beam. The kick factor is defined so that $Nr_e\kappa_t y_0/\gamma$ gives the deflection angle for the bunch, with N being the number of particles in the bunch, r_e – the classical electron radius, and y_0 – the beam offset. Using a result of Ref. [3] we can express κ_t in terms of $\mathrm{Re}\, Z_t$,

$$\kappa_t = \int_0^\infty d\omega F\left(\frac{\omega\sigma_z}{c}\right) \mathrm{Re}\, Z_t(\omega), \tag{41}$$

where

$$F(x) = -\frac{i}{\pi} e^{-x^2} \mathrm{erf}(ix). \tag{42}$$

Putting Eq. (40) in Eq. (41) and using the relation

$$\int_0^\infty \frac{dx}{x} F(x) = \frac{1}{2} \tag{43}$$

we find for the kick factor of a taper

$$\kappa_t = \frac{2(1 - b_1^4/b_2^4)}{b_1^2}. \tag{44}$$

Interestingly, that in the limit $b_2 \gg b_1$ this result reduces to the kick of a diaphragm of radius b_1 [11]. We see that in the diffraction regime the wake generated by a tapered collimator is not suppressed compared to the rectangular iris of the same radius.

Similar to the consideration at the end of Section 5, we can easily obtain the radiated energy Eq. (38) using the notion of the electromagnetic field "scraped off" by the collimator. Assuming that the incident electromagnetic field of the beam current in the annulus $b_1 < \rho < b_2$ is converted into radiation after reflection in the lateral wall of the entrance collimator, we find the average Poynting vector

$$S = \frac{c}{8\pi}(\boldsymbol{E}^0)^2, \tag{45}$$

where $\boldsymbol{E}^0$ is given by Eq. (32),

$$S = \frac{I_0^2\Delta^2}{2\pi c}\left(\frac{1}{b^4} + \frac{1}{b_2^4}\right). \tag{46}$$

The energy flow in the annulus is given by the integral

$$\int_{b_1}^{b_2} 2\pi\rho d\rho S = \frac{I_0^2\Delta^2}{2b_1^2 c}\left(1 - \frac{b_1^4}{b_2^4}\right), \tag{47}$$

and is exactly equal to the result given by Eq. (38).

7 Flat collimator, intermediate regime

The geometry of a flat collimator is shown in Fig. 2 where b_1 and b_2 are now the half-gaps in the vertical direction. We will use two coordinate systems below: x, y, z, and r, θ, x, with x directed along the wide side of the collimator.

Analogous to the field (32) in the straight section of a round collimator, which gives a zero-order approximation to the problem, we need an expression for the electric field of a dipole current inside a rectangular straight pipe of cross section $2b_2 \times 2h$, with $h \gg b_2$. A good approximation for the field is

given by the limit $h \to \infty$, that is the case of two parallel plates located at distance $2b_2$. This field is given by the gradient of the potential function ϕ

$$E_x^0 = -\frac{\partial \phi}{\partial x}, \qquad E_y^0 = -\frac{\partial \phi}{\partial y}, \tag{48}$$

where

$$\phi(x,y) = \frac{\pi I_0 \Delta}{c b_2} \frac{\sin \frac{\pi y}{b_2}}{\cosh \frac{\pi x}{b_2} - \cos \frac{\pi y}{b_2}} e^{ikz}. \tag{49}$$

The magnetic field of the beam is $\boldsymbol{H}^0 = \hat{\boldsymbol{z}} \times \boldsymbol{E}^0$, where $\hat{\boldsymbol{z}}$ is the unit vector in the direction of the z axis.

Inside the taper the field given by Eqs. (48) and (49) does not satisfy the boundary conditions. As in the previous Section, we represent the field inside the taper as a sum $\boldsymbol{E} = \boldsymbol{E}^{\rm rad} + \boldsymbol{E}^0$, where $\boldsymbol{E}^{\rm rad}$ is the radiation electric field.

In the intermediate regime, as was explained in Section 2, the radiated field will be a combination of TE_{0n} eigenmodes. For a large-aspect ratio small-angle taper, $h \gg b$ and $\alpha \ll 1$, and in the limit of high frequencies $kr \gg 1$, the field in these modes is

$$\begin{aligned} E_\theta &= \pm \frac{k k_r}{\sqrt{r}} e^{\pm i k_r r} \cos \frac{\pi n x}{h}, \\ H_r &= \mp \frac{i n \pi k_r}{h \sqrt{r}} e^{\pm i k_r r} \sin \frac{\pi n x}{h}, \\ H_x &= \frac{k_r^2}{\sqrt{r}} e^{\pm i k_r r} \cos \frac{\pi n x}{h}, \end{aligned} \tag{50}$$

where $k_r = \sqrt{k^2 - (\pi n/h)^2}$, x is the coordinate measured along the wide side (h) of the taper, and n is an odd number. The upper (lower) sign corresponds to the modes propagating in the negative (positive) direction of the z axis. In these modes the magnetic field is an antisymmetric function of x; we discarded the modes with the symmetric dependance of H_r because they are not excited due to the symmetry of the problem. The norm for TE_{0n} modes is

$$N_n = \frac{\alpha c h k k_r^3}{2\pi}, \tag{51}$$

and the energy flow $P_n = \frac{1}{4} N_n$.

We will see from what follows that the typical value of n is such that $n \sim \sqrt{kh^2/r} \gg 1$. This means that, first, the excited modes propagate through

the collimator without being reflected from the narrow aperture. Second, the wavenumber k_r for the modes is close to k, and can be approximately calculated as $k_r \approx k - \pi^2 n^2/2kh^2$.

The magnetic current at the walls of the taper has two components, $i_x^{\rm mag} = (c/4\pi)E_r^0|_{\rm wall}$ and $i_r^{\rm mag} = -(c/4\pi)E_x^0|_{\rm wall}$. The signs in these equations are valid for the upper side of the taper, $y = b(z)$, — for the lower side $i^{\rm mag}$ changes sign because of the opposite direction of the unit vector $\boldsymbol{n}$ in Eq. (12). Note that E_x^0 is much larger than E_r^0 which is of the order of αE_x^0, hence $i_x^{\rm mag} \sim \alpha i_r^{\rm mag}$. Calculations show that in the scalar product $\boldsymbol{i}_{\rm mag}\boldsymbol{H}$ the dominant contribution comes from the $i_r^{\rm mag}H_r$ term. This gives for the amplitude a_n^+ of the waves propagating in the direction of the beam

$$a_n^+ = -\frac{2}{N_n}\int_{-\infty}^{\infty} dx \int_{r_1}^{r_2} dr i_r^{\rm mag} H_r, \tag{52}$$

where $i_r^{\rm mag}$ is calculated for the upper plate of the collimator, $y = b(z)$, and the factor of 2 takes into account an equal contribution from the lower plate. The magnetic field H_r in Eq. (52) is given by Eq. (50) with the upper sign, corresponding to the modes propagating in the negative direction.

The radial component of the magnetic current as a function of coordinates r, x is

$$i_r^{\rm mag} = \frac{c}{4\pi}E_x^0|_{y=b(z)} = \frac{\pi I_0 \Delta}{4b_2^2}\frac{\sin\frac{\pi b(r)}{b_2}\sinh\frac{\pi x}{b_2}}{\left(\cos\frac{\pi b(r)}{b_2} - \cosh\frac{\pi x}{b_2}\right)^2} e^{-ikr\cos\alpha}. \tag{53}$$

One can see that for a typical value of $n \sim \sqrt{kh^2/r}$ the wavelength of the excited modes in the x direction is of the order of $2\sqrt{r/k} \gg b$. Since the function $i_r^{\rm mag}$ is localized in the x direction within $\Delta x \sim 1/b$, we can Taylor expand $\sin(\pi n x/h)$ and keep only the linear term of the expansion, $\sin(n\pi x/h) \approx n\pi x/h$. Then integration over x can be performed analytically using the following relation

$$\int_{-\infty}^{\infty} d\xi \frac{\xi \sinh\xi}{(\cos\zeta - \cosh\xi)^2} = 2\frac{\pi - \zeta}{\sin\zeta}. \tag{54}$$

Using also approximations $\cos\alpha \approx 1$ and $k_r \approx k - n^2\pi^2/2kh^2$ one arrives at the following result

$$a_n^+ = \frac{2in^2\pi^3\Delta I_0}{cb_2h^3k^3\alpha}\int_{r_1}^{r_2} dr \frac{b_2 - b(r)}{\sqrt{r}} e^{-in^2\pi^2 r/2h^2 k}. \tag{55}$$

The dominant contribution to this integral comes from the region $0 < n \lesssim n_{\max}$ where $n_{\max}$ is determined from the condition that the phase factor in Eq. (55) becomes of the order of one, $n_{\max} \sim \sqrt{kh^2/r}$. We used this estimate above as a characteristic value of n for the radiated modes.

The total energy radiated from the taper is given by a sum over all modes

$$P_\omega = \sum_{\text{odd}\, n} P_n |a_n^+|^2 \approx \frac{1}{2} \int_0^\infty dn P_n |a_n^+|^2. \tag{56}$$

After explicit integration over n, the result can be represented in the following form

$$P_\omega = \frac{c\pi^{1/2} k^{1/2} I_0^2 \Delta^2}{2\alpha c} I, \tag{57}$$

where

$$I = \int_{r_1}^{r_2} \left(\frac{1 - b(s_1)/b_2}{\sqrt{s_1}} \right)' \left(\frac{1 - b(s_2)/b_2}{\sqrt{s_2}} \right)' \frac{ds_1 ds_2}{\sqrt{|s_1 - s_2|}}, \tag{58}$$

and the prime stands for the derivative with respect to the argument s_1 or s_2, respectively. In the limit $r_2 \gg r_1$ (which also means $b_2 \gg b_1$) this integral can be simplified

$$I \approx \frac{1}{4 r_1^{3/2}} \int_1^\infty \frac{ds_1 ds_2}{(s_1 s_2)^{3/2} \sqrt{|s_1 - s_2|}} = \frac{2}{3 r_1^{3/2}}. \tag{59}$$

In this limit, P_ω is

$$P_\omega = \frac{c\pi^{1/2} k^{1/2} I_0^2 \Delta^2 \alpha^{1/2}}{3 b_1^{3/2} c}. \tag{60}$$

Repeating calculation of the previous section (see Eqs. (39) and (40)), we can now find the real part of the transverse impedance of the full collimator

$$\mathrm{Re}\, Z_t = 2 \times \frac{4\pi^{1/2} \alpha^{1/2}}{3 k^{1/2} b_1^{3/2} c}, \tag{61}$$

where an additional factor 2 takes into account the two tapers. Using Eq. (41) one can now find the transverse kick for a Gaussian bunch:

$$\kappa_t = 2.7 \frac{\alpha^{1/2}}{\sigma_z^{1/2} b_1^{3/2}}. \tag{62}$$

Note that this result is valid in the case when both tapers are adjacent to each other.

8 Flat collimator, diffraction regime

To calculate the impedance in the diffraction regime, we will use a simple energy flow argument developed at the end of Sections 5 and 6. To simplify calculations, we assume that $b_2 \gg b_1$, which reduces Eq. (48) to

$$E_x^0 = \frac{4I_0\Delta}{c}\frac{xy}{(x^2+y^2)^2}e^{ikz}, \qquad E_y^0 = \frac{4I_0\Delta}{c}\frac{y^2-x^2}{(x^2+y^2)^2}e^{ikz}. \tag{63}$$

During the passage through the collimator, the beam field is now "scraped off" in the area $b_1 < |y| < b_2$ and since b_2 is assumed large, we can take the limit $b_2 \to \infty$. The power lost by the beam for a single taper is

$$P_\omega = 2\int_{b_1}^{\infty} dy \int_{-\infty}^{\infty} \frac{c}{8\pi}[(E_x^0)^2 + (E_y^0)^2]dx. \tag{64}$$

The integration yields

$$P_\omega = \frac{\Delta^2 I_0^2}{4cb_1^2}, \tag{65}$$

which is exactly half of the result Eq. (38) for the round collimator in the limit $b_2 \gg b_1$.

We conclude, that the impedance (kick factor) of the flat collimator in the diffraction regime is equal to half of the impedance (kick factor) for the round collimator with the same minimal gap b_1.

9 Conclusion

In this paper we extended the analysis of previous studies to cover all possible regimes of the high-frequency impedance of tapered collimators.

For round collimators, Yokoya's formula, given by Eq. (1) is valid in the limit of small angles α. Increasing the angle brings the impedance into diffraction regime, with the real part of Z_t given by Eq. (40). In this regime, the impedance is close to that of an iris with the same aperture, and hence tapering does not suppress the wake. The kick factor in this regime is given by Eq. (44); it does not depend on the bunch length.

For rectangular collimators with a large width to height ratio, the inductive regime given by Eq. (3) is only valid if the applicability condition Eq. (4) is satisfied. Larger angles correspond to the intermediate regime, where

the beam radiation becomes important. The real part of the impedance and the kick factor in this regime are given by Eq. (61) and Eq. (62), respectively. The kick factor in the intermediate regime scales with the bunch length as $\sigma_z^{-1/2}$. Further increase of the angle brings the system into the diffraction regime with the impedance equal to half of the impedance of the round collimator in the diffraction regime.

10 Acknowledgements

I would like to thank K. Bane, S. Heifets and R. Warnock for numerous discussions of the subject of this paper.

11 Appendix

Consider the integral

$$I = \int_{x_1}^{x_2} dx f(x) H_\nu^{(1)}(x) e^{-ix\cos\alpha}, \tag{66}$$

where $f(x)$ is a smooth function of its argument. We will use the asymptotic representation of the Hankel function valid for $x \gg \nu$

$$H_\nu^{(1)}(x) \approx \left(\frac{2}{\pi x}\right)^{1/2} e^{i\psi(x)}, \tag{67}$$

where the phase $\psi(x)$ satisfies the equation

$$\frac{d\psi}{dx} = \left(1 - \frac{\nu^2}{x^2}\right)^{1/2} \approx 1 - \frac{\nu^2}{2x^2}. \tag{68}$$

For small α, $\cos\alpha \approx 1 - \alpha^2/2$, and

$$I \approx \left(\frac{2}{\pi}\right)^{1/2} \int_{x_1}^{x_2} \frac{dx}{\sqrt{x}} f(x) e^{i\zeta(x)}, \tag{69}$$

where $\zeta(x) = \psi(x) - x(1 - \alpha^2/2)$.

In the stationary phase method, the dominant contribution to the integral comes from the point where $\zeta'(x) = 0$. Using Eq. (68) we find the location of the stationary point

$$x = x_0 \equiv \frac{\nu}{\alpha}. \tag{70}$$

Note that $x_0/\nu \sim \alpha^{-1} \gg 1$, which justifies the asymptotic representation of H_ν in Eq. (67). If x_0 lies within the integration interval, $x_1 < x_0 < x_2$, a standard calculation of the stationary-point integral gives

$$I \approx \frac{2}{\alpha} f\left(\frac{\nu}{\alpha}\right) e^{i\zeta(\nu/\alpha)+i\pi/4}. \tag{71}$$

If x_0 is located outside of the interval $[x_1, x_2]$, the value of the integral will be much smaller than that given by Eq. (71), and we can approximate $I \approx 0$.

We can now find the condition when the stationary point method approach is valid. The size of the interval δx where the dominant contribution to the integral comes from, $\delta x \sim |\zeta''(x_0)|^{-1/2} \sim (\nu/\alpha^3)^{1/2}$, must be much smaller than the value of x_0. Since $\delta x/x \sim (\alpha\nu)^{-1/2} \sim (\alpha^2 x_0)^{-1/2}$, the condition $\delta x/x \ll 1$ is fulfilled if

$$\alpha^2 x \sim \alpha b k \gg 1, \tag{72}$$

which is the condition of the diffraction regime Eq. (5).

References

[1] The NLC Design Group, *Zeroth-Order Design Report for the Next Linear Collider*, Report SLAC-474, Stanford Linear Accelerator Center, Stanford, CA, USA (May 1996).

[2] K. Yokoya, *Impedance of Slowly Tapered Structures*, Tech. Rep. SL/90-88 (AP), CERN (1990).

[3] G. V. Stupakov, Particle Accelerators **56**, 83 (1996).

[4] G. V. Stupakov, *Geometrical wake of a smooth flat collimator*, Tech. Rep. SLAC-PUB-7167, SLAC (May 1996).

[5] P. Tenenbaum, in *2001 Particle Accelerator Conference, Chicago, 2001.*

[6] G. V. Stupakov, in *2001 Particle Accelerator Conference, Chicago, 2001.*

[7] G. V. Stupakov, Phys. Rev. ST Accel. Beams **1**, 064401 (1998).

[8] A. W. Chao, *Physics of Collective Beam Instabilities in High Energy Accelerators* (Wiley, New York, 1993).

[9] L. A. Vainshtein, *Electromagnetic Waves* (Radio i svyaz', Moscow, 1988), in Russian.

[10] R. E. Collin, *Field Theory of Guided Waves* (IEEE Press, New York, 1991), 2nd ed.

[11] F. Zimmermann, K. L. F. Bane, and C. K. Ng, in *Proc. European Particle Accelerator Conference, Sitges, 1996* (IOP, Bristol, 1996).